J. Fluid Mech. (2026), *vol.* 1043, R5, doi:10.1017/jfm.2026.12056



Semi-analytical eddy-viscosity and backscattering closures for 2-D geophysical turbulence

Yifei Guan[1,2] **and Pedram Hassanzadeh**[1]

[1]University of Chicago, Chicago, IL 60637, USA

[2]Union College, Schenectady, NY 12308, USA

Corresponding author: Yifei Guan, guany@union.edu

(Received 4 June 2026 UTC; revised 5 August 2026 UTC; accepted 20 August 2026 UTC)

Physics-based eddy-viscosity and backscattering closures are widely used for large-eddy simulation (LES) of geophysical turbulence, but their key parameters are often chosen empirically. Here, we develop a semi-analytical framework for estimating these parameters in two-dimensional (2-D) geophysical turbulence by adapting a Lilly-type scaling argument. Specifically, we obtain closed-form estimates, up to an amplitude constant, for the coefficients of the Leith and Smagorinsky eddy-viscosity closures, a biharmonic eddy-viscosity closure and the Jansen–Held backscattering closure with a prescribed backscattering fraction. The amplitude constant appears in the turbulent kinetic energy direct-cascade spectrum and can be diagnosed from a few direct numerical simulation (DNS) or eddy-resolving snapshots. For isotropic cases ($\beta = 0$), the diagnosed amplitude constant is consistent with previous theoretical estimates based on closure, renormalisation-group and mode-coupling methods. The resulting semi-analytical parameters closely match the online-learned values obtained using ensemble Kalman inversion across several 2-D geophysical turbulence set-ups (Guan *et al. Phys. Rev. Res.* vol. 8, 2026, p. 023215). LES using these parameters reproduces key DNS statistics, including the tails of the vorticity distribution, and robustly outperforms dynamic Leith and Smagorinsky baselines.

Key words: turbulence modelling, homogeneous turbulence, geophysical and geological flows

1. Introduction

Subgrid-scale (SGS) closures are essential for large-eddy simulation (LES) of turbulent flows in the Earth system, where DNS is computationally infeasible (Meneveau &

© The Author(s), 2026. Published by Cambridge University Press. This is an Open Access article, distributed under the terms of the Creative Commons Attribution licence (https://creativecommons.org/licenses/by/4.0/), which permits unrestricted re-use, distribution and reproduction, provided the original article is properly cited.

https://doi.org/10.1017/jfm.2026.12056 Published online by Cambridge University Press

Katz 2000; Pearson *et al.* 2017; Ross *et al.* 2023; Bracco *et al.* 2025). SGS closures are commonly categorised as structural or functional models (Sagaut 2006). Structural closures can accurately represent SGS stress structures, but may suffer from numerical instabilities and filter dependence (Leonard 1975; Clark *et al.* 1979; Zanna & Bolton 2020; Jakhar *et al.* 2024). Our recent work showed that including higher-order terms can yield stable and accurate LES of 2-D geophysical turbulence (Jakhar *et al.* 2026). However, this approach requires high-LES resolution. Functional closures, including eddy-viscosity and backscattering models, target the net energy and/or enstrophy transfer across the filter and can be effective at lower LES resolutions (Smagorinsky 1963; Leith 1996; Jansen & Held 2014; Jansen *et al.* 2015; Perezhogin *et al.* 2019; Perezhogin 2020; Grooms 2023). Related closure-theory studies have developed scale-dependent eddy-viscosity and backscatter parametrisations for 2-D and geophysical turbulence (Kraichnan 1976; Frederiksen & Davies 1997; Kitsios *et al.* 2013).

Unlike the three-dimensional (3-D) Smagorinsky coefficient, which can be related to the Kolmogorov constant, the corresponding constants for 2-D geophysical LES closures have remained largely empirical. Data-driven approaches have recently been used to optimise LES closure parameters from statistical data (Mons *et al.* 2021). In our recent work, we used ensemble Kalman inversion (EKI) to learn closure parameters for eight set-ups of 2-D geophysical turbulence (Guan *et al.* 2026). The optimal parameters were found to be nearly constant across cases with different flow regimes, and LES using these parameters outperformed common and dynamic-closure baselines. This raises a natural question: are the learned near-universal parameters merely empirical or can they be explained by classical 2-D turbulence theory?

In this note, we present, to the best of our knowledge, the first semi-analytical framework for deriving closure parameters for 2-D geophysical turbulence from turbulence scaling. This framework also provides a physical interpretation of the near-universal parameters previously obtained via EKI-based online learning (Guan *et al.* 2026). Specifically, we semi-analytically estimate C_L, C_S and C_{JH} from the turbulent kinetic energy (TKE) direct-cascade scaling law $\hat{E}(k) = A\eta^{2/3}k^{-3}$, where k is wavenumber, η is the enstrophy dissipation rate and A is an amplitude constant (Kraichnan 1967; Leith 1968; Batchelor 1969). We further derive the corresponding coefficients for the log-corrected spectrum $\hat{E}(k) = A'\eta^{2/3}k^{-3}[\ln(k/k_f)]^{-1/3}$ and for a general power law $\hat{E}(k) = A''\eta^{2/3}(k_*)^{p-3}k^{-p}$. Since A, A' and A'' are obtained from DNS or high-fidelity spectra, the approach is semi- rather than fully analytical. As discussed later, estimates of the amplitude constants A, A' and A'' from DNS agree with previous theoretical works (Kraichnan 1967, 1971; Olla 1991; Nandy & Bhattacharjee 1995). The resulting parameters closely match the EKI-optimised values and yield LES that reproduce key DNS statistics, suggesting that the previously learned optimal parameters are not merely empirical fits, but can be interpreted through classical 2-D turbulence theory.

2. DNS, LES and closures

We consider the dimensionless 2-D β-plane vorticity equation (e.g. Vallis 2017)

$$\frac{\partial \omega}{\partial t} + \mathcal{J}(\omega, \psi) = \frac{1}{Re}\nabla^2\omega - f - r\omega + \beta\frac{\partial \psi}{\partial x}, \qquad \nabla^2\psi = -\omega. \tag{2.1}$$

Here, $\mathcal{J}$ is the Jacobian, $f(x, y) = k_f[\cos(k_f x) + \cos(k_f y)]$ is a time-independent deterministic forcing at wavenumber k_f, Re is the Reynolds number, β is the planetary-vorticity-gradient parameter and $r = 0.1$ is the linear friction coefficient.

https://doi.org/10.1017/jfm.2026.12056 Published online by Cambridge University Press

Applying a sharp spectral cutoff filter, denoted by $\overline{(\cdot)}$, gives the LES or filtered-DNS (FDNS) equation

$$\frac{\partial \overline{\omega}}{\partial t} + \mathcal{J}(\overline{\omega}, \overline{\psi}) = \frac{1}{Re}\nabla^2\overline{\omega} - \overline{f} - r\overline{\omega} + \beta\frac{\partial \overline{\psi}}{\partial x} - \underbrace{\left[\overline{\mathcal{J}(\omega, \psi)} - \mathcal{J}(\overline{\omega}, \overline{\psi})\right]}_{\Pi^{SGS} = \nabla\times(\nabla\cdot\tau^{SGS})}, \quad \nabla^2\overline{\psi} = -\overline{\omega}. \tag{2.2}$$

The SGS term Π^{SGS} stems from the Jacobian and must be closed in terms of the resolved variables $(\overline{\psi}, \overline{\omega})$. For eddy-viscosity closures,

$$\tau^{SGS} = -2\nu_e\overline{\mathcal{S}}, \tag{2.3}$$

where $\overline{\mathcal{S}}$ is the resolved strain-rate tensor. The Smagorinsky model uses

$$\nu_e = (C_S\Delta)^2\langle\overline{\mathcal{S}}^2\rangle^{1/2}, \tag{2.4}$$

while the Leith model uses

$$\nu_e = (C_L\Delta)^3\langle(\nabla\overline{\omega})^2\rangle^{1/2}, \quad \text{with} \quad \Delta = L/N_{LES}. \tag{2.5}$$

Here, $L = 2\pi$ is the domain length, N_{LES} is the number of grid points in each direction and Δ is the filter width. Additionally, $\langle\cdot\rangle$ denotes domain averaging. The Jansen–Held (JH) closure model is written as

$$\Pi^{SGS} = \nabla^2(\nu_e\nabla^2\overline{\omega}) + \nu_B\nabla^2\overline{\omega}, \tag{2.6}$$

where the first term dissipates enstrophy through biharmonic eddy viscosity and the second term re-injects energy by anti-diffusion. Similar to their original papers (Jansen & Held 2014; Jansen *et al.* 2015), we use

$$\nu_e = (C_{JH}\Delta)^6\left\langle(\nabla^2\overline{\omega})^2\right\rangle^{1/2}, \quad \nu_B = -C_B\frac{\left\langle\overline{\psi}\nabla^2(\nu_e\nabla^2\overline{\omega})\right\rangle}{\left\langle\overline{\psi}\nabla^2\overline{\omega}\right\rangle}. \tag{2.7}$$

The parameter C_B prescribes the fraction of dissipated energy re-injected into the resolved scales. Following previous studies (Jansen & Held 2014; Guan *et al.* 2026), we set $C_B = 0.95$ in all cases. In the following, we derive the semi-analytical expression for scalar coefficients C_L, C_S and C_{JH}.

3. Semi-analytical derivation of the closure parameters

The derivation in the following is, to the best of our knowledge, the first Lilly-type global scaling argument for estimating scalar coefficients in commonly used 2-D eddy-viscosity and backscattering closures. We treat the eddy viscosity as spatially uniform, $\nu_e = \nu_e(t)$, so the resulting coefficients should be interpreted as scalar, domain-averaged closure constants rather than local eddy-viscosity fields. The cutoff condition $\Delta \sim L_\eta$ is imposed up to a proportionality constant that is absorbed into the closure coefficient. A sharp spectral cutoff, $k_c = \pi/\Delta$, is used throughout. Detailed derivations and extensions to a general k^{-p} scaling law are given in the supplementary material.

3.1. k^{-3} *spectrum scaling*

In 2-D turbulence, the interscale enstrophy transfer is

$$\eta = \langle\bar{\omega}\Pi\rangle, \tag{3.1}$$

https://doi.org/10.1017/jfm.2026.12056 Published online by Cambridge University Press

where $\eta > 0$ denotes transfer from resolved to subgrid or dissipative scales. For an eddy-viscosity closure $\Pi = -\nu_e \nabla^2 \bar{\omega}$ with spatially uniform $\nu_e(t)$,

$$\eta = -\nu_e \langle \bar{\omega} \nabla^2 \bar{\omega} \rangle = \nu_e \langle (\nabla \bar{\omega})^2 \rangle. \tag{3.2}$$

Requiring Δ to resolve the enstrophy-dissipation scale $L_\eta \sim \nu_e^{1/2} \eta^{-1/6} \sim \nu_e^{1/3} \langle (\nabla \bar{\omega})^2 \rangle^{-1/6}$ (Batchelor 1969; Boffetta 2007; Boffetta & Musacchio 2010) gives the Leith form

$$\nu_e = (C_L \Delta)^3 \langle (\nabla \bar{\omega})^2 \rangle^{1/2}. \tag{3.3}$$

Combining (3.2) and (3.3) yields

$$\eta = (C_L \Delta)^3 \langle (\nabla \bar{\omega})^2 \rangle^{3/2}. \tag{3.4}$$

Using the direct-cascade TKE spectrum

$$\hat{E}(k) = A \eta^{2/3} k^{-3} \tag{3.5}$$

(Kraichnan 1967; Leith 1968; Batchelor 1969) and Parseval's theorem,

$$\langle (\nabla \bar{\omega})^2 \rangle = 2 \int_0^{k_c} k^4 \hat{E}(k) \, \mathrm{d}k = A \eta^{2/3} k_c^2, \tag{3.6}$$

where $k_c = \pi / \Delta$. Here and in the following, the scaling law is applied to the FDNS spectrum up to k_c. For moments dominated by high wavenumbers, the error from extending the direct-cascade form below k_f is assumed small. Substitution into (3.4) gives

$$C_L = \pi^{-1} A^{-1/2}. \tag{3.7}$$

To the best of our knowledge, (3.7) gives the first explicit relation between a 2-D LES closure coefficient and the amplitude of an enstrophy-cascade scaling law. In the following, the same framework is extended to Smagorinsky, biharmonic eddy-viscosity and JH backscattering closures. For the biharmonic eddy-viscosity part of the JH closure, setting $C_B = 0$,

$$\eta = \nu_e \langle \bar{\omega} \nabla^4 \bar{\omega} \rangle = \nu_e \langle (\nabla^2 \bar{\omega})^2 \rangle, \qquad \nu_e = (C_{JH} \Delta)^6 \langle (\nabla^2 \bar{\omega})^2 \rangle^{1/2}. \tag{3.8}$$

The corresponding spectral moment is

$$\langle (\nabla^2 \bar{\omega})^2 \rangle = 2 \int_0^{k_c} k^4 \hat{Z}(k) \, \mathrm{d}k = \frac{A}{2} \eta^{2/3} k_c^4, \tag{3.9}$$

where $\hat{Z}(k) = k^2 \hat{E}(k)$ is the enstrophy spectrum. Substituting back into (3.8) and using $k_c = \pi / \Delta$ gives

$$C_{JH} = (A/2)^{-1/4} \pi^{-1}. \tag{3.10}$$

In general, for a $2m$-order eddy-viscosity model ($\Pi = (-1)^m \nu_e \nabla^{2m} \bar{\omega}$ and $\nu_e = (C_m \Delta)^{3m} \langle (\nabla^m \bar{\omega})^2 \rangle^{1/2}$), the model coefficient can be derived as $C_m = (A/m)^{-1/(2m)} / \pi$. As discussed by Kitsios *et al.* (2013), higher k_c may favour a higher-order operator.

For the full JH model with a prescribed C_B, using (2.6) in (3.2) gives

$$\eta = (C_{JH} \Delta)^6 (A/2)^{3/2} \eta k_c^6 - \nu_B A \eta^{2/3} k_c^2. \tag{3.11}$$

From (2.7),

$$\nu_B = C_B \nu_e \frac{2 \int_0^{k_c} k^2 \hat{Z}(k) \, \mathrm{d}k}{2 \int_0^{k_c} \hat{Z}(k) \, \mathrm{d}k} \approx C_B \nu_e \frac{k_c^2}{2 \ln(k_c)}, \tag{3.12}$$

https://doi.org/10.1017/jfm.2026.12056 Published online by Cambridge University Press

where the denominator is evaluated from the smallest nonzero wavenumber, $k = 1$, in the 2π-periodic domain. This logarithmic factor introduces a weak dependence on the large-scale cutoff and on the sharp-filter convention. Substituting (3.12) into (3.11) gives

$$C_{JH} = (A/2)^{-1/4}\pi^{-1}\left(1 - \frac{C_B}{\ln(k_c)}\right)^{-1/6}. \tag{3.13}$$

Finally, we estimate C_S by matching the globally averaged Smagorinsky and Leith eddy viscosities for a resolved field with the assumed spectrum:

$$(C_L\Delta)^3\langle(\nabla\bar{\omega})^2\rangle^{1/2} = (C_S\Delta)^2\langle\bar{\mathcal{S}}^2\rangle^{1/2}. \tag{3.14}$$

With

$$\langle\bar{\mathcal{S}}^2\rangle = 2\int_0^{k_c} k^2\hat{E}(k)\,\mathrm{d}k \approx 2A\eta^{2/3}\ln(k_c), \tag{3.15}$$

we obtain

$$C_S = A^{-3/4}\pi^{-1}(2\ln(k_c))^{-1/4}. \tag{3.16}$$

Equations (3.7), (3.13) and (3.16) give semi-analytical expressions for the Leith, JH and Smagorinsky coefficients under the classical k^{-3} enstrophy-cascade scaling, all determined up to the amplitude constant A. To the best of our knowledge, this provides the first explicit scaling-based estimate of these commonly used 2-D LES closure coefficients. We next repeat the derivation using the logarithmically corrected k^{-3} spectrum.

3.2. $k^{-3}[\ln(k/k_f)]^{-1/3}$ *spectrum scaling*

For the logarithmically corrected direct-cascade spectrum (Kraichnan 1971)

$$\hat{E}(k) = A'\eta^{2/3}k^{-3}[\ln(k/k_f)]^{-1/3}, \tag{3.17}$$

the scaling is applied only for $k > k_f$; in the discrete spectra, we therefore use $k_f + 1$ as the lower limit. The leading-order spectral moments are

$$\begin{aligned}\langle(\nabla\bar{\omega})^2\rangle &\approx 2\int_{k_f+1}^{k_c} A'\eta^{2/3}k[\ln(k/k_f)]^{-1/3}\,\mathrm{d}k\\ &\approx A'\eta^{2/3}k_c^2[\ln(k_c/k_f)]^{-1/3}\end{aligned} \tag{3.18}$$

and

$$\begin{aligned}\langle(\nabla^2\bar{\omega})^2\rangle &\approx 2\int_{k_f+1}^{k_c} A'\eta^{2/3}k^3[\ln(k/k_f)]^{-1/3}\,\mathrm{d}k\\ &\approx \frac{A'}{2}\eta^{2/3}k_c^4[\ln(k_c/k_f)]^{-1/3}.\end{aligned} \tag{3.19}$$

These approximations follow from the slow variation of the logarithmic factor or, equivalently, from Karamata's theorem (Bingham *et al.* 1989). Repeating the above-mentioned balances gives

$$C_L' = \frac{1}{\pi A'^{1/2}}[\ln(k_c/k_f)]^{1/6}, \tag{3.20}$$

$$C_{JH}' = (A'/2)^{-1/4}\pi^{-1}[\ln(k_c/k_f)]^{1/12}. \tag{3.21}$$

https://doi.org/10.1017/jfm.2026.12056 Published online by Cambridge University Press

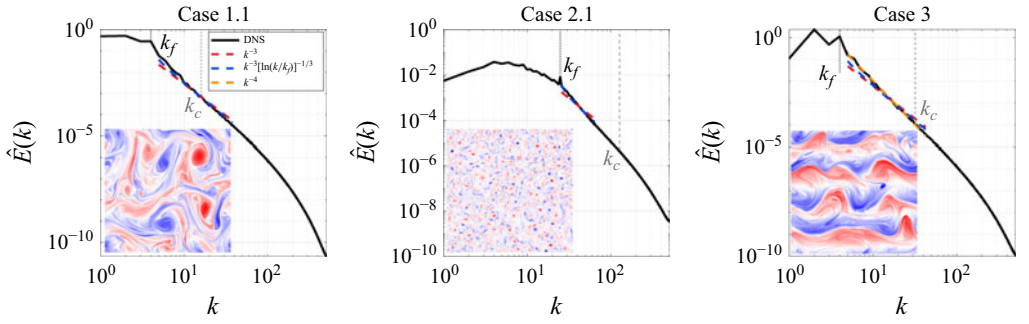


Figure 1. TKE spectra ($\hat{E}(k)$) and examples of ω for representative Cases 1.1, 2.1 and 3. The k_f and k_c are marked. The black curves show DNS spectra averaged over 100 snapshots. The red (blue) dashed line shows the k^{-3} scaling law (with logarithmic correction), with the A (A') values shown in table 1. The orange dashed line shows the effective k^{-4} scaling law for Case 3 only. With a sharp spectral cutoff filter, the FDNS spectrum overlaps with the DNS spectrum over $k \in [0, k_c]$.

Here, we use C'_L and C'_{JH} with $'$ to denote coefficients derived from the logarithmically corrected direct-cascade spectrum. For a prescribed C_B, the same asymptotic estimate gives $\nu_B \approx (C_B/3)\nu_e k_c^2[\ln(k_c/k_f)]^{-1}$, leading to

$$C'_{JH} = (A'/2)^{-1/4}\pi^{-1}[\ln(k_c/k_f)]^{1/12}\left(1 - \frac{2C_B}{3\ln(k_c/k_f)}\right)^{-1/6}. \tag{3.22}$$

Similarly, matching the globally averaged Smagorinsky and Leith eddy viscosities yields

$$C'_S = 3^{-1/4}A'^{-3/4}\pi^{-1}. \tag{3.23}$$

3.3. *Effective k^{-4} scaling for the β-plane case*

For the anisotropic β-plane case considered in the following, the angle-integrated TKE spectrum is steeper than the classical k^{-3} direct-cascade spectrum, as shown in figure 1. We therefore also use an effective k^{-4} scaling,

$$\hat{E}(k) = A''\eta^{2/3}k_* k^{-4}, \tag{3.24}$$

where k_* is a characteristic wavenumber used to keep A'' dimensionless and the choice of k_* will affect the value of A'', but will not affect the derived closure coefficients. Following the same arguments and assumptions as before, and using the leading-order spectral moments

$$\langle(\nabla\bar{\omega})^2\rangle \approx 2A''\eta^{2/3}k_* k_c, \qquad \langle(\nabla^2\bar{\omega})^2\rangle \approx \frac{2A''}{3}\eta^{2/3}k_* k_c^3, \tag{3.25}$$

we obtain the Leith coefficient and JH coefficient with prescribed C_B:

$$C''_L = \frac{1}{\pi}\left(\frac{k_c}{2A''k_*}\right)^{1/2}, \quad C''_{JH} = \frac{1}{\pi}\left(\frac{2A''k_*}{3}\right)^{-1/4}k_c^{1/4}\left(1 - \frac{3C_B k_1}{k_c}\right)^{-1/6}. \tag{3.26}$$

Here, k_1 denotes the lowest nonzero wavenumber and equals 1 in a $2\pi \times 2\pi$ computational domain. We use C''_L and C''_{JH} with $''$ to denote coefficients derived from the effective k^{-4} scaling. These expressions are used only as an effective isotropic representation of the angle-integrated spectrum in the anisotropic β-plane case. The corresponding C''_S involves a strain moment that is dominated by k_1, and it is more sensitive to the chosen fitting range

https://doi.org/10.1017/jfm.2026.12056 Published online by Cambridge University Press

Case	1.1	1.2	1.3	1.4	2.1	2.2	2.3	3
Numerical and physical set-up								
Re	20 000	20 000	100 000	300 000	20 000	100 000	300 000	20 000
β	0	0	0	0	0	0	0	20
k_f	4	4	4	4	25	25	25	4
k_c	16	32	128	128	128	128	128	32
k^{-3} prediction								
A	2.1 (0.21)	2.1 (0.21)	1.7 (0.017)	1.8 (0.046)	2.7 (0.090)	2.1 (0.013)	1.9 (0.027)	2.8 (0.28)
C_L	0.21 (0.010)	0.21 (0.010)	0.23 (0.0011)	0.23 (0.0029)	0.19 (0.0031)	0.21 (0.00066)	0.22 (0.0015)	0.18 (0.010)
C_S	0.11 (0.0087)	0.11 (0.0082)	0.11 (0.00085)	0.11 (0.0021)	0.084 (0.0020)	0.099 (0.00046)	0.10 (0.0011)	0.089 (0.0075)
C_{JH}	0.33 (0.0083)	0.33 (0.0082)	0.34 (0.00082)	0.33 (0.0021)	0.30 (0.0025)	0.32 (0.00049)	0.33 (0.0011)	0.30 (0.0083)
Log-corrected prediction								
A'	2.2 (0.21)	2.2 (0.21)	2.1 (0.020)	2.4 (0.066)	2.0 (0.061)	2.0 (0.010)	2.0 (0.026)	2.9 (0.27)
C'_L	0.22 (0.010)	0.24 (0.011)	0.26 (0.0013)	0.25 (0.0035)	0.24 (0.0036)	0.24 (0.00061)	0.24 (0.0015)	0.20 (0.010)
C'_S	0.13 (0.0095)	0.13 (0.0095)	0.13 (0.0010)	0.12 (0.0026)	0.14 (0.0031)	0.14 (0.00053)	0.14) (0.0013)	0.10 (0.0081)
C'_{JH}	0.35 (0.0084)	0.35 (0.0084)	0.35 (0.00087)	0.34 (0.0024)	0.35 (0.0026)	0.35 (0.00045)	0.35 (0.0011)	0.32 (0.0080)
EKI-optimised (online learned)								
C_L^{EKI}	0.23 (0.032)	0.25 (0.028)	0.26 (0.028)	0.24 (0.025)	0.24 (0.026)	0.23 (0.024)	0.21 (0.035)	0.21 (0.015)
C_S^{EKI}	0.12 (0.012)	0.12 (0.010)	0.11 (0.0041)	0.12 (0.0082)	0.12 (0.008)	0.12 (0.011)	0.10 (0.015)	0.10 (0.012)
C_{JH}^{EKI}	0.34 (0.019)	0.32 (0.010)	0.33 (0.0043)	0.30 (0.0064)	0.32 (0.0051)	0.32 (0.0036)	0.31 (0.010)	0.31 (0.014)

Table 1. Physical and numerical parameters of the eight cases and comparison between semi-analytical predictions and EKI-optimised coefficients. The semi-analytical predictions are obtained using either the k^{-3} scaling or the logarithmically corrected $k^{-3}[\ln(k/k_f)]^{-1/3}$ scaling. Values in parentheses denote one standard deviation over the 100 DNS TKE spectra. For the JH closure, C_{JH} is estimated with $C_B = 0.95$ for all semi-analytical predictions. For the anisotropic β-plane Case 3, the effective k^{-4} scaling predicts $C''_L = 0.18(0.0079)$ and $C''_{JH} = 0.32(0.0070)$. The DNS and LES set-up details, and the derivation of C''_S (not used as primary estimate) are in the supplementary material.

than the Leith and biharmonic estimates. Therefore, it is not used as a primary coefficient estimate.

4. Numerical results

To evaluate the semi-analytical estimates of C_L, C_{JH} and C_S, we use the DNS and LES datasets generated by Guan *et al.* (2026). The physical and numerical parameters of the eight cases are summarised in table 1. The DNS TKE spectra and representative vorticity fields for three cases are shown in figure 1. Table 1 also reports the diagnosed amplitudes A and A' obtained by fitting $\hat{E}(k) = A\eta^{2/3}k^{-3}$ and $\hat{E}(k) = A'\eta^{2/3}k^{-3}[\ln(k/k_f)]^{-1/3}$ to the direct-cascade range $k \in [k_f + 1, k_\eta]$ of the DNS TKE spectra. In 2-D turbulence, the enstrophy-cascade dissipation wavenumber scales as $k_{diss} \sim \nu^{-1/2}\eta^{1/6} \sim Re^{1/2}\eta^{1/6}$

https://doi.org/10.1017/jfm.2026.12056 Published online by Cambridge University Press

(Boffetta 2007; Boffetta & Musacchio 2010). To avoid fitting the viscous-dissipation range, we set the fitting upper bound to $k_\eta = \xi Re^{1/2}\eta^{1/6}$ with $\xi = 0.25$. Here, ξ is a fitting-range parameter, chosen conservatively and tested by sensitivity analysis in the supplementary material available at https://doi.org/10.1017/jfm.2026.12056. The enstrophy dissipation rate is diagnosed from the same DNS TKE spectra as (Davidson 2015)

$$\eta = \langle(\nabla\omega)^2\rangle/Re = \frac{2}{Re}\int_0^{k_{DNS}} k^4\hat{E}(k)\,\mathrm{d}k. \tag{4.1}$$

After the flow reaches statistical equilibrium, the snapshot-averaged spectrum and the diagnosed mean η are statistically stationary. The TKE spectrum is calculated by averaging spectra from 100 decorrelated DNS snapshots. As discussed by Guan *et al.* (2026), even one snapshot can be sufficient for estimating A and A' accurately. Except for Case 3, A and A' are nearly flow independent and are both close to 2. The somewhat larger A in Case 2.1 is likely related to the shorter available fitting interval between $k_f + 1$ and k_η, making the original k^{-3} scaling more sensitive to the selected fitting upper bound. This motivates the log-corrected scaling, which shows reduced sensitivity to ξ in the supplementary material. The diagnosed values of A' are close to the mode-coupling estimates of the log-corrected 2-D enstrophy-cascade spectral constant reported by Nandy & Bhattacharjee (1995), including the corrected one-loop value 1.923 and the self-consistent value 2.201, and are broadly consistent with other theoretical estimates based on test-field closure approximation and renormalisation-group methods (e.g. Kraichnan 1971; Olla 1991). The diagnosed A values are consistent with empirical effective k^{-3} amplitudes reported in 2-D turbulence (e.g. Boffetta & Ecke 2012; Gupta *et al.* 2019). Case 3 has larger fitted amplitudes ($A = 2.8$ and $A' = 2.9$), likely due to the strong anisotropy and jet-like structures induced by the β effect. As shown in figure 1, the k^{-3} and log-corrected k^{-3} spectra are too shallow for this case. We therefore also consider an effective k^{-4} scaling of the angle-integrated spectrum for Case 3. This scaling should be interpreted as an empirical isotropic representation of the steepened spectrum in the anisotropic β-plane case, rather than as a universal β-plane scaling law (e.g. Rhines 1975; Galperin *et al.* 2008, 2010; Sukoriansky *et al.* 2009). Physically, the imposed planetary vorticity gradient supports Rossby-wave dynamics and anisotropic jet-like organisation, which redistribute energy towards large-scale zonal modes and weaken the assumptions of a k^{-3} enstrophy cascade. Here, the k^{-4} estimation is intended as a consistency check showing how the coefficient-estimation framework changes for a steeper observed spectrum, rather than as evidence of improvement. Since only one anisotropic case is considered, universality of the effective exponent and amplitude in anisotropic regimes is left for future work.

Overall, the semi-analytical estimates of C_L, C_{JH} and C_S agree well with the EKI-optimised values of Guan *et al.* (2026). This agreement provides an independent validation of the semi-analytical approach and, furthermore, shows that the EKI-optimised parameters can be interpreted through classical 2-D turbulence scaling. LES results using the semi-analytically estimated parameters for three representative cases are shown in figure 2. These cases are selected to represent distinct regimes and to include cases where the semi-analytical predictions deviate most from the EKI-optimised values. In *a posteriori* tests based on TKE spectra and vorticity probability density functions, LES with the semi-analytical parameters robustly outperform the dynamic Leith (Maulik & San 2016) and dynamic Smagorinsky (Germano *et al.* 1991) baselines, particularly in the probability density function (p.d.f.) tails (additional implementation details are provided in the supplementary material). The backscattering JH closures better capture the tails of the FDNS vorticity p.d.f.s than purely diffusive closures.

https://doi.org/10.1017/jfm.2026.12056 Published online by Cambridge University Press

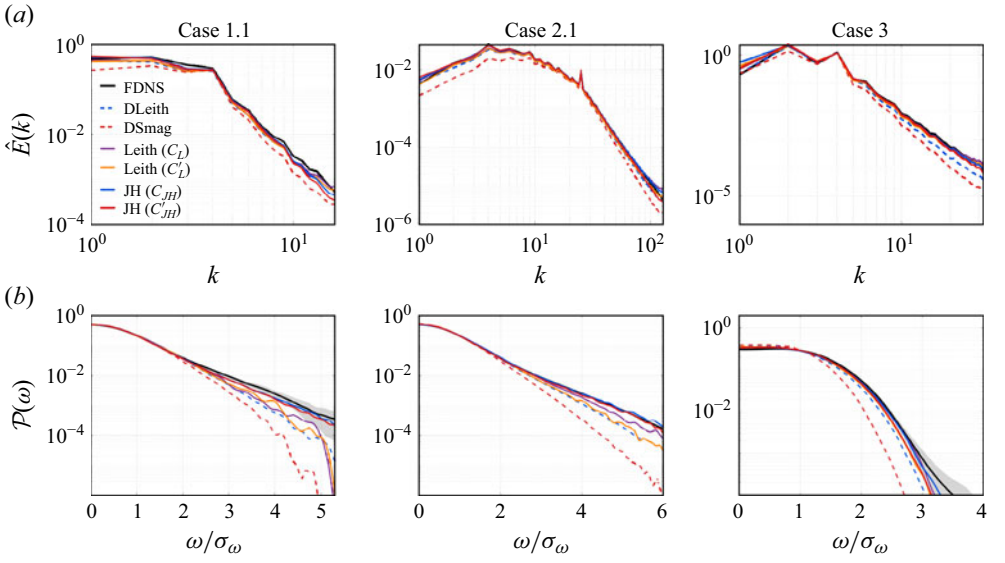


Figure 2. *A posteriori* testing with semi-analytical model parameters shown in table 1. (*a*) TKE spectra ($\hat{E}(k)$) comparison among the ground truth (FDNS), baseline models (dynamic Leith, or DLeith, and dynamic Smagorinsky, or DSmag) and the semi-analytical models derived from the k^{-3} scaling (with C_L or C_{JH}), and the logarithmic correction (with C'_L or C'_{JH}), for representative Cases 1.1, 2.1 and 3. The semi-analytical models show a better match with the ground truth than DSmag among all three cases and better than DLeith in Case 3. (*b*) Positive tail of the vorticity probability density function, $\mathcal{P}(\omega)$. The negative tail gives the same qualitative conclusions because the vorticity is nearly symmetric about zero. The semi-analytical JH models consistently match the FDNS $\mathcal{P}(\omega)$ within 1 standard deviation (grey shaded area), especially in the tails or rare extreme events. The semi-analytical Leith models, although not as accurate as the JH models, outperform the baseline models. The mild high-k curl-up of Case 2.1 $\hat{E}(k)$ may be improved with a higher-order operator with an estimated C_m.

5. Summary and conclusion

We have developed semi-analytical estimates for the scalar coefficients in the Leith, Smagorinsky and Jansen–Held closures for 2-D geophysical turbulence. The derivation extends a Lilly-type global scaling argument to 2-D turbulence and uses either the classical k^{-3} direct-cascade spectrum or its log-corrected form above the forcing scale.

The estimates depend on an amplitude constant, e.g. A or A', and are therefore semi-analytical rather than fully analytical. For $\beta = 0$ cases, however, the diagnosed amplitudes are nearly case-independent. Specifically, the log-corrected amplitude is consistent with previous theoretical estimates based on test-field closure approximations, renormalisation-group analysis, and mode-coupling theory. The resulting closure coefficients agree well with the EKI-optimised parameters obtained in our online-learning study (Guan *et al.* 2026).

A posteriori LES tests show that closures using the semi-analytical parameters reproduce key DNS statistics and compare favourably with dynamic Leith and Smagorinsky baselines, especially in the vorticity-p.d.f. tails. For the anisotropic β-plane case, the angle-integrated spectrum is steeper and is better represented by an effective k^{-4} scaling, which should be viewed as a first approximation rather than a universal β-plane law. Future work will test these coefficients in more realistic geophysical models and develop an anisotropic theory for β-plane regimes with a sweep on Re, k_f, etc. More broadly, together with the EKI results of Guan *et al.* (2026), this work illustrates how

https://doi.org/10.1017/jfm.2026.12056 Published online by Cambridge University Press

modern data-driven closure discovery can motivate, guide and validate new theoretical developments in turbulence modelling.

Supplementary material. Supplementary material is available at https://doi.org/10.1017/jfm.2026.12056.

Acknowledgements. We thank Pavel Perezhogin for insightful discussions.

Funding. This work was supported by NSF grant OAC-2005123 and by Schmidt Sciences, LLC. Computational resources were provided by ACCESS (ATM170020) and CISL (URIC0004).

Declaration of interests. The authors report no conflict of interest.

References

Batchelor, G.K. 1969 Computation of the energy spectrum in homogeneous two-dimensional turbulence. *Phys. Fluids* **12** (12), II–233.

Bingham, N.H., Goldie, C.M. & Teugels, J.L. 1989 *Regular Variation*, vol. 27. Cambridge University Press.

Boffetta, G. 2007 Energy and enstrophy fluxes in the double cascade of two-dimensional turbulence. *J. Fluid Mech.* **589**, 253–260.

Boffetta, G. & Ecke, R.E. 2012 Two-dimensional turbulence. *Annu. Rev. Fluid Mech.* **44**, 427–451.

Boffetta, G. & Musacchio, S. 2010 Evidence for the double cascade scenario in two-dimensional turbulence. *Phys. Rev. E* **82** (1), 016307.

Bracco, A., Brajard, J., Dijkstra, H.A., Hassanzadeh, P., Lessig, C. & Monteleoni, C. 2025 Machine learning for the physics of climate. *Nat. Rev. Phys.* **7** (1), 6–20.

Clark, R.A., Ferziger, J.H. & Reynolds, W.C. 1979 Evaluation of subgrid-scale models using an accurately simulated turbulent flow. *J. Fluid Mech.* **91** (1), 1–16.

Davidson, P.A. 2015 *Turbulence: an Introduction for Scientists and Engineers*. Oxford University Press.

Frederiksen, J.S. & Davies, A.G. 1997 Eddy viscosity and stochastic backscatter parameterizations on the sphere for atmospheric circulation models. *J. Atmos. Sci.* **54** (20), 2475–2492.

Galperin, B., Sukoriansky, S. & Dikovskaya, N. 2008 Zonostrophic turbulence. *Phys. Scr.* **T132**, 014034.

Galperin, B., Sukoriansky, S. & Dikovskaya, N. 2010 Geophysical flows with anisotropic turbulence and dispersive waves: flows with a β-effect. *Ocean Dyn.* **60**, 427–441.

Germano, M., Piomelli, U., Moin, P. & Cabot, W.H. 1991 A dynamic subgrid-scale eddy viscosity model. *Phys. Fluids A* **3** (7), 1760–1765.

Grooms, I. 2023 Backscatter in energetically-constrained Leith parameterizations. *Ocean Model.* **186**, 102265.

Guan, Y., Hassanzadeh, P., Schneider, T., Dunbar, O., Huang, D.Z., Wu, J. & Lopez-Gomez, I. 2026 Online learning of eddy-viscosity and backscattering closures for geophysical turbulence using ensemble Kalman inversion. *Phys. Rev. Res.* **8** (2), 023215.

Gupta, A., Jayaram, R., Chaterjee, A.G., Sadhukhan, S., Samtaney, R. & Verma, M.K. 2019 Energy and enstrophy spectra and fluxes for the inertial-dissipation range of two-dimensional turbulence. *Phys. Rev. E* **100** (5), 053101.

Jakhar, K., Guan, Y. & Hassanzadeh, P. 2026 Analytical and AI-discovered stable, accurate, and generalizable subgrid-scale closure for geophysical turbulence. *Phys. Rev. Lett.* **136** (6), 064201.

Jakhar, K., Guan, Y., Mojgani, R., Chattopadhyay, A. & Hassanzadeh, P. 2024 Learning closed-form equations for subgrid-scale closures from high-fidelity data: promises and challenges. *J. Adv. Model. Earth Syst.* **16** (7), e2023MS003874.

Jansen, M.F. & Held, I.M. 2014 Parameterizing subgrid-scale eddy effects using energetically consistent backscatter. *Ocean Model.* **80**, 36–48.

Jansen, M.F., Held, I.M., Adcroft, A. & Hallberg, R. 2015 Energy budget-based backscatter in an eddy permitting primitive equation model. *Ocean Model.* **94**, 15–26.

Kitsios, V., Frederiksen, J.S. & Zidikheri, M. 2013 Scaling laws for parameterisations of subgrid eddy–eddy interactions in simulations of oceanic circulations. *Ocean Model.* **68**, 88–105.

Kraichnan, R.H. 1967 Inertial ranges in two-dimensional turbulence. *Phys. Fluids* **10** (7), 1417–1423.

Kraichnan, R.H. 1971 Inertial-range transfer in two-and three-dimensional turbulence. *J. Fluid Mech.* **47** (3), 525–535.

Kraichnan, R.H. 1976 Eddy viscosity in two and three dimensions. *J. Atmos. Sci.* **33** (8), 1521–1536.

Leith, C. 1996 Stochastic models of chaotic systems. *Physica D* **98** (2–4), 481–491.

https://doi.org/10.1017/jfm.2026.12056 Published online by Cambridge University Press

LEITH, C.E. 1968 Diffusion approximation for two-dimensional turbulence. *Phys. Fluids* **11** (3), 671–672.
LEONARD, A. 1975 Energy cascade in large-eddy simulations of turbulent fluid flows. In *Advances in Geophysics*, vol. 18, pp. 237–248. Elsevier.
MAULIK, R. & SAN, O. 2016 Dynamic modeling of the horizontal eddy viscosity coefficient for quasigeostrophic ocean circulation problems. *J. Ocean Engng Sci.* **1**, 300–324.
MENEVEAU, C. & KATZ, J. 2000 Scale-invariance and turbulence models for large-eddy simulation. *Annu. Rev. Fluid Mech.* **32** (1), 1–32.
MONS, V., DU, Y. & ZAKI, T.A. 2021 Ensemble-variational assimilation of statistical data in large-eddy simulation. *Phys. Rev. Fluids* **6** (10), 104607.
NANDY, M.K. & BHATTACHARJEE, J.K. 1995 Mode-coupling theory, dynamic scaling, and two-dimensional turbulence. *Intl J. Mod. Phys. B* **9** (09), 1081–1097.
OLLA, P. 1991 Renormalization-group analysis of two-dimensional incompressible turbulence. *Phys. Rev. Lett.* **67** (18), 2465.
PEARSON, B., FOX-KEMPER, B., BACHMAN, S. & BRYAN, F. 2017 Evaluation of scale-aware subgrid mesoscale eddy models in a global eddy-rich model. *Ocean Model.* **115**, 42–58.
PEREZHOGIN, P.A. 2020 2D turbulence closures for the barotropic jet instability simulation. *Russ. J. Numer. Anal. Model.* **35** (1), 21–35.
PEREZHOGIN, P.A., GLAZUNOV, A.V. & GRITSUN, A.S. 2019 Stochastic and deterministic kinetic energy backscatter parameterizations for simulation of the two-dimensional turbulence. *Russ. J. Numer. Anal. Model.* **34** (4), 197–213.
RHINES, P.B. 1975 Waves and turbulence on a beta-plane. *J. Fluid Mech.* **69** (3), 417–443.
ROSS, A., LI, Z., PEREZHOGIN, P., FERNANDEZ-GRANDA, C. & ZANNA, L. 2023 Benchmarking of machine learning ocean subgrid parameterizations in an idealized model. *J. Adv. Model. Earth Syst.* **15** (1), e2022MS003258.
SAGAUT, P. 2006 *Large Eddy Simulation for Incompressible Flows*. Springer Science & Business Media.
SMAGORINSKY, J. 1963 General circulation experiments with the primitive equations: I. The basic experiment. *Mon. Weath. Rev.* **91** (3), 99–164.
SUKORIANSKY, S., DIKOVSKAYA, N. & GALPERIN, B. 2009 Transport of momentum and scalar in turbulent flows with anisotropic dispersive waves. *Geophys. Res. Lett.* **36** (14), L14609.
VALLIS, G.K. 2017 *Atmospheric and Oceanic Fluid Dynamics*. Cambridge University Press.
ZANNA, L. & BOLTON, T. 2020 Data-driven equation discovery of ocean mesoscale closures. *Geophys. Res. Lett.* **47** (17), e2020GL088376.

https://doi.org/10.1017/jfm.2026.12056 Published online by Cambridge University Press